A microstructurally motivated description of the deformation of vertically aligned carbon nanotube structures

Shelby B. Hutchens, Alan Needleman, and Julia R. Greer

Citation: Appl. Phys. Lett. **100**, 121910 (2012); doi: 10.1063/1.3697686

View online: http://dx.doi.org/10.1063/1.3697686

View Table of Contents: http://apl.aip.org/resource/1/APPLAB/v100/i12

Published by the American Institute of Physics.

A microstructurally motivated description of the deformation of vertically aligned carbon nanotube structures

Shelby B. Hutchens,[1] Alan Needleman,[2] and Julia R. Greer[1,a)]
[1]*Materials Science, California Institute of Technology, 1200 E. California Blvd., Pasadena, California 91125, USA*
[2]*Materials Science and Engineering, University of North Texas, 1155 Union Circle #305310, Denton, Texas 76203, USA*

(Received 17 February 2012; accepted 7 March 2012; published online 23 March 2012)

Vertically aligned carbon nanotube's extreme compliance and mechanical energy absorption/dissipation capabilities are potentially promising aspects of their multi-functionality. Mathematical models have revealed that a hardening-softening-hardening material relation can capture the unique sequential, periodic buckling behavior displayed by vertically aligned carbon nanotubes under uniaxial compression. Yet the physical origins of these models remain unknown. We provide a microstructure-based motivation for such a phenomenological constitutive relation and use it to explore changes in structural response with nanotube volume fraction. © *2012 American Institute of Physics*. [http://dx.doi.org/10.1063/1.3697686]

The collective properties of carbon nanotubes in the form of vertically aligned carbon nanotubes (VACNTs) have been explored for applications ranging from micro-electro-mechanical system (MEMS)[1–3] to low temperature energy dissipating materials.[4–6] This has led to growing interest in developing an understanding of VACNT's mechanical response which is key for rational design and life cycle analysis.[1–3,5,7–13]

VACNT materials are complex, hierarchical, and largely disordered assemblies of carbon nanotubes (CNTs) aligned nominally vertically with respect to the growth substrate. Experimental investigations have found that VACNTs have mechanical energy dissipative properties,[4,5,7,10] can exhibit high recoverability after large strains,[8,14,15] and deform via a sequential periodic buckling mechanism under uniaxial compression.[1,2,7,8,11] While observations of these behaviors are numerous, the physical mechanisms governing them remain poorly understood. To date, only a few mathematical models have been proposed and those either numerically replicate aspects of the structural response without taking into account underlying mechanisms[16,17] or describe only the linear elastic and viscoelastic response.[2,8,10] What is lacking is a physically motivated hypothesis from which predictions of structural behavior can be made given systematic variation of material properties.

This report introduces a microstructure-based motivation for a previously proposed constitutive relation[17] that captured the formation of sequential, periodic, and localized buckles in cylindrical VACNT pillars subjected to uniaxial compression (Figure 1(a)). We propose that this constitutive relation can be motivated and manipulated by the superposition of microstructure-driven behavior from two known characteristics of VACNTs, their foam-like structure, and the attractive interactions between CNTs. Several groups have shown that VACNTs deform similarly to foams.[2,7,8] This behavior is thought to arise from the open-cell structure created by interwoven and intertwined tubes, which act as supporting struts (Fig. 1(b)). In addition, CNTs are known to be inherently "sticky" with attractive inter-tube forces arising via van der Waals interactions.[18–20] We use the composite relation generated by these two material behaviors to predict the VACNT structural response as a function of volume fraction of nanotubes.

We will connect this composite stress-strain response to the form of the constitutive relation described in detail in Hutchens *et al.*[17] Briefly, the latter relation is a three-dimensional elastic-viscoplastic Mises type relation modified to account for plastic compressibility. Elastic deformation is assumed to be isotropic and is governed by Young's modulus, E, and elastic Poisson's ratio, ν. The viscoplastic deformation rate is a function of the plastic strain rate and a plastic Poisson's ratio. The plastic strain rate is modeled using a strain rate sensitivity expression, $\dot{\varepsilon}_p = \dot{\varepsilon}_0[\sigma_e/g(\varepsilon_p)]^{1/m}$, with $\dot{\varepsilon}_0$ being a reference strain rate, m the strain rate sensitivity factor, and $g(\varepsilon_p)$ the piecewise, hardening function having the form

$$\frac{g(\varepsilon_p)}{\sigma_0} = \begin{cases} 1 + h_1\varepsilon_p & \varepsilon_p < \varepsilon_1 \\ 1 + h_1\varepsilon_1 & \\ \quad + h_2(\varepsilon_p - \varepsilon_1) & \varepsilon_1 < \varepsilon_p < \varepsilon_2 \\ 1 + h_1\varepsilon_1 + h_2(\varepsilon_2 - \varepsilon_1) & \\ \quad + h_3(\varepsilon_p - \varepsilon_2) & \varepsilon_p > \varepsilon_2 \end{cases} . \quad (1)$$

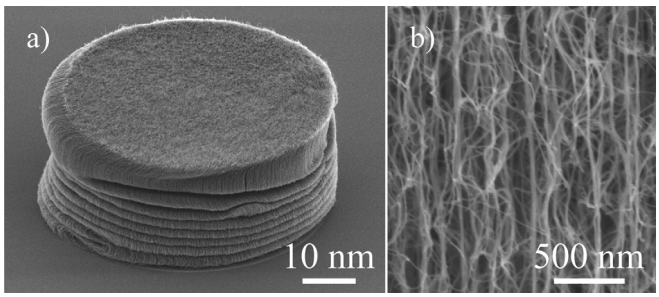

FIG. 1. (a) Scanning electron micrograph of a 50 μm diameter VACNT pillar after uniaxial compression to ~80% strain, showing irrecoverable sequential periodic buckling. (b) Magnified image illustrating the open, foam-like microstructure of VACNTs.

a)Electronic mail: jrgreer@caltech.edu.

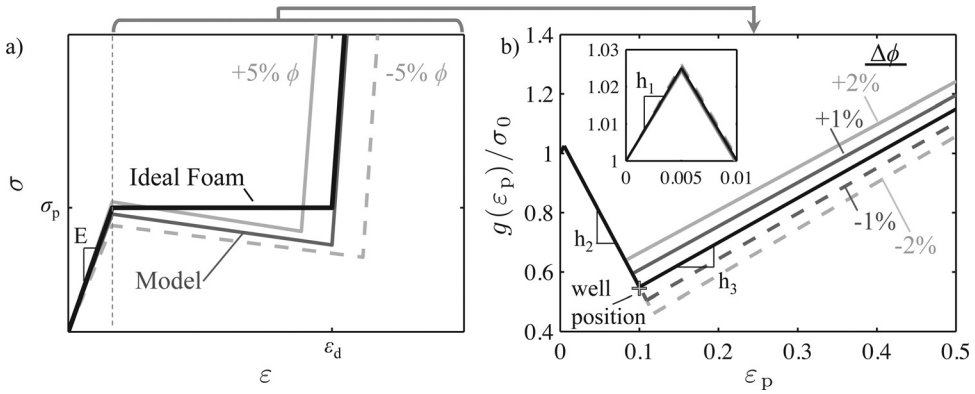

FIG. 2. (a) Idealized foam behavior (black solid) contrasted with the proposed model (dark gray solid) which allows for softening. Effects of ±5% changes in tube volume fraction, ϕ, are shown by the lighter solid and dashed lines, respectively. (b) Plastic hardening function and the effects of ±1% and 2% changes in ϕ shown by the light gray solid and dashed lines, respectively. Note that σ_0 (y-axis) is also a function of ϕ. The "plus" symbol corresponds to the well position (parameters used (black): $\varepsilon_1 = 0.005, \varepsilon_2 = 0.1, h_1 = 5.0, h_2 = -5.0$, and $h_3 = 1.5$).

Selecting positive values for h_1 and h_3, and a negative value for h_2 results in a hardening-softening-hardening relation (Figure 2(b)). More details are provided in Hutchens *et al.*[17] The aim of the model proposed herein is to relate E and $g(\varepsilon_p)$ to the pre-deformation relative density, or volume fraction, of the VACNT material.

Starting with the foam-like nature of VACNTs, we look to the idealized behavior of cellular solids which is highly dependent on material density, ρ, and is expressed as a function of the relative density of the structure, ρ/ρ_s, where the subscript "s" refers to the properties of the strut material. Using relations developed by Gibson and Ashby,[21] we write the basic formulation for an open-cell ideal elastic foam as shown in Figure 2(a). It is comprised of (1) elastic behavior at small strains, (2) a plateau corresponding to the buckling of individual struts and compaction of the material, and (3) the onset of densification. This piecewise material response, governed by the elastic modulus, plateau stress, σ_{pl}, and densification strain, ε_d, varies with relative density according to the following relationships:[21]

$$\frac{E}{E_s} = C\left(\frac{\rho}{\rho_s}\right)^2, \quad \sigma_{pl} = C'\left(\frac{\rho}{\rho_s}\right)^2, \quad \varepsilon_d = 1 - \alpha\left(\frac{\rho}{\rho_s}\right), \quad (2)$$

where $C \approx 1, C' \approx 0.05$, and α varies between 1.4 and 2.0. This formulation provides a prediction of the material stress-strain response for changes in relative density, ρ/ρ_s, which is equivalent to strut volume fraction, ϕ. (Note that the third of Eq. (2) is only valid for $\rho/\rho_s < 1/\alpha$ or ε_d becomes negative ($\phi < 0.7 - 0.5$). We are well within this limit with VACNTS, $\phi \sim 0.13$.)[8] Constants, C and C' are unimportant because here we consider only relative changes in ϕ. We choose $\alpha = 1.4$.[21] Notably, no softening exists in the idealized foam relation, analogous to $h_2 = 0$ in Eq. (1), which displays no localized buckle formation.[17]

We augment the idealized foam framework by incorporating an energy reduction associated with the CNT struts coming into increasing contact with one another during compression. This is expected to occur only during the elastic and plateau regimes; during densification, the inter-strut contact levels off. We formulate a simple term that quantifies the increase in strut contact (and reduction in energy) as a function of increasing strain. Following arguments similar to those used by van der Waals in the treatment of attractive interactions between molecules,[22] we begin with a single material element consisting of a length of tube in a box of volume, V. For a length of tube, L, having radius, r, the probability of a random point selected within that box lying within the tube is $L\pi r^2/V$. The probability that any point in the box intersects the tube twice is an "and" statement or the single intersection probability squared. (Note that excluded volume is not accounted for, unlike in van der Waals' treatment.) Therefore, the volume of tube crossover within the box/material element is $V_{\text{intersect}} = (L\pi r^2/V)^2 V = \phi_V^2 V$, where $L\pi r^2/V$ equals the volume fraction of tube at that volume, ϕ_V. We argue, as van der Waals did, that to first approximation the energy of interaction between tubes is proportional to this crossover volume. Thus, for some interaction energy per unit volume, $a > 0$, the energy arising from tube-tube interactions, U, is expressed in the intensive as

$$U/V \propto -a\phi_V^2. \quad (3)$$

Using the definition of volume fraction, we write ϕ_V in terms of the initial volume, V_0, and initial volume fraction, ϕ, as $\phi_V = \phi(V_0/V)$. Under hydrostatic strain, changes in the volume of the element, V, written in terms of the stretch ratio, λ, are given by $V = V_0\lambda^3$. Therefore, substituting this relation, the expression for ϕ_V, and the relation between stretch ratio and true strain, $\varepsilon = \ln(\lambda)$, into Eq. (3), we obtain an expression for the intensive energy decrease arising from tube interactions as a function of strain

$$U/V \propto -a\phi^2 e^{3\varepsilon}. \quad (4)$$

We obtain the stress from the first derivative of Eq. (4) with respect to ε. Since the initial state of the VACNT material element includes some finite amount of inter-tube contact, the relative change in stress is obtained by subtracting the initial stress state at $\varepsilon = 0$. Performing these two operations on Eq. (4) yields an expression for the stress applied to the material element due to attractive tube-tube interactions, $\sigma_{\text{interact}} \propto a\phi^2(e^{3\varepsilon} - 1)$. Given the values we use for ε_2, it is reasonable to simplify further using a Taylor series expansion around $\varepsilon = 0$ and discarding higher order terms to obtain a linear dependence on ε

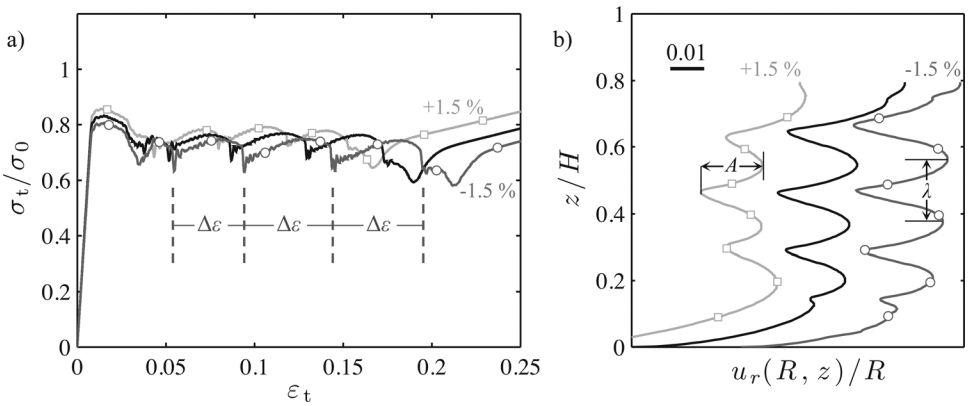

FIG. 3. (a) True stress (σ_t)–true strain (ε_t) responses for the initial (black), $+1.5\%\phi$ (squares/lighter), and $-1.5\%\phi$ (circles/darker) cases with an illustration of $\Delta\varepsilon$. (b) Series of outer displacement profiles of the axisymmetric cylinder for the initial (black), $+1.5\%\phi$ (squares/lighter), and $-1.5\%\phi$ (circles/darker) cases with illustrations of amplitude, A, and wavelength, λ. The position (u_r, z) of the outer surface of the pillar is normalized by the undeformed pillar radius, R, and height, H.

$$\sigma_{\text{interact}} \propto -a\phi^2\varepsilon. \tag{5}$$

This is superimposed upon the idealized foam framework to produce a simplified, piecewise constitutive relation analogous to that given by Eq. (1) and described in Hutchens *et al.*[17] The series approximation has an average error of ~1% up to a strain of 0.12 (our largest value of ε_2).

Note two key assumptions of this development. First, we do not expect all of the material softening to be accounted for by attractive inter-tubular interactions. Softening would also be expected to arise from, for example, a loss of stiffness due to individual tube buckling. However, by assuming a value for a, we can achieve any desired strain-softening during the plateau regime for the material element, while determining how that softening slope reacts to changes in ϕ (Fig. 2(a)). Second, the above arguments are energy based. In applying the stress-strain relation developed from these arguments to the viscoplastic relation, we make the assumption that the plastic dissipation qualitatively exhibits the same dependence on volume fraction as the stored energy.

In previous work, we showed that sequential buckling only occurred within a particular range of "well" positions (Fig. 2(b)) of the hardening relation.[17] Therefore, we select a well position in the center of this region as the reference point around which to perform volume fraction perturbations. Each section of the hardening relation, $g(\varepsilon_p)$, as well as the Young's modulus, E, in the original framework relation is subject to a volume fraction dependence as described by Eqs. (2) and (5). Parameters correlate between the model and constitutive relation as follows. The Young's modulus is the sum of the ideal foam dependence (the first of Eq. (2)) plus the interaction stress (Eq. (5)) and therefore, $E \propto \phi^2$. σ_{pl} is analogous to the σ_0, and therefore scales as, $\sigma_0 \propto \phi^2$. The short initial portion of $g(\varepsilon_p)$ in the hardening relation, defined by h_1 and ε_1 (inset, Fig. 2(b)), is for continuity in the transition from elastic-to-plastic behavior and has no corresponding feature in the foam-based model. We keep it constant with respect to volume fraction changes. The softening slope, h_2, behaves according to Eq. (5), $h_2\sigma_0 \propto \phi^2$. Variation in the well location, given by ε_3, correlates to ε_d (the third of Eq. (2)) and follows $\varepsilon_3 = 1 - 1.4\phi$. The final slope of the hardening relation, h_3, corresponds to densification in the composite relation and is independent of ϕ.

We explore the implications of this microstructurally driven constitutive relation by varying the volume fraction of tubes by $\pm 0.5\% - 2.0\%$. Representative hardening function input curves are shown in Fig. 2(b). Figure 3(a) shows the resulting output stress-strain response for the initial and $\pm 1.5\%$ ϕ cases. We quantify the response in two ways: (1) amplitude, A, and wavelength, w, of buckles at a true strain of $\varepsilon_t = 0.23$ taken from the outer displacement profiles (Figure 3(b)) and (2) strain increments between buckling events, $\Delta\varepsilon$, taken from the stress-strain response (Fig. 3(a)). These measurements are summarized in Figure 4.

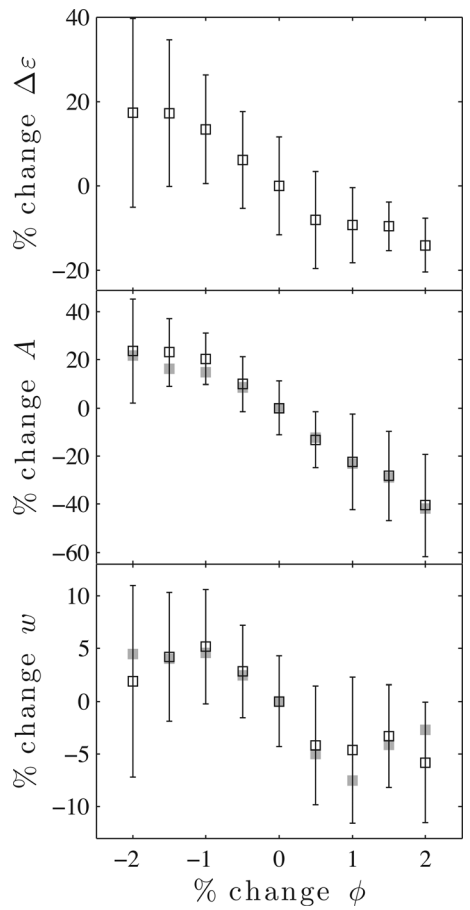

FIG. 4. Characteristic measurements showing decreased buckle length scales with increases in ϕ. All data are plotted as percent differences from the initial case. Top: changes in strain between stress drops. Middle: changes in buckle amplitude. Bottom: changes in buckle wavelength. Error bars are obtained from the standard deviation in measurements over 3 buckles for $\Delta\varepsilon$ and over 6 half buckle wavelengths for A and w. Gray, solid points indicate measurements obtained through sine wave fits of the outer displacement profile (Fig. 3(b)).

We find that larger ϕ results in the overall decrease of every length scale characteristic of buckle formation: A, w, and $\Delta\varepsilon$. The effect of ϕ on each of these characteristics is significant, with 1%–2% changes in ϕ driving 20% variations in $\Delta\varepsilon$ and 40% variations in amplitude. Changes in the wavelength are less marked but follow a trend similar to $\Delta\varepsilon$ and A. The extent of variation in ϕ is limited by the relatively small parameter space eliciting buckling, likely due to the isotropic formulation of our constitutive model.[17]

Physically, the effect of ϕ on buckling characteristics can be understood as follows. The largest change in the constitutive relation with ϕ (Fig. 2(b)) is in the densification strain (ε_2) which varies linearly. Large horizontal shifts in the well position directly impact the local flow behavior of the model,[17] just as the onset of densification would in a real foam. Thus, lower volume fraction corresponds to a slower onset of localized densification. This leads to less frequent triggering of new buckling events which means the formation of longer buckles capable of accommodating more strain by increasing in amplitude. The decreasing softening slope at lower ϕ only slightly mitigates the effect by providing less drive for localized flow due to decreased instability.

In summary, we have proposed a microstructure-based motivation for a hardening-softening-hardening constitutive relation previously shown to capture key qualitative features of VACNT cylinder compression experiments. The motivation for this relation stems from considering the energetics of inter-tube interactions together with an idealized cellular-solid mathematical description and describes a dependence of Young's modulus and viscoplastic hardening on nanotube volume fraction. The model is, of course, idealized. Effects of density variations on Poisson's ratio are not accounted for nor are the possible effects of nanotube buckling on softening. Nevertheless, the model permits us to explore the effects of nanotube volume fraction on characteristic length scales describing buckle formation. The model predicts that the amplitude, wavelength, and strain increment between buckles all increase with reduced volume fraction and provides a starting point for developing improved material models for VACNTs.

This work was supported by the Institute for Collaborative Biotechnologies through grant W911NF-09-0001 from the U.S. Army Research Office. The content of the information does not necessarily reflect the position or the policy of the Government, and no official endorsement should be inferred.

[1]O. Yaglioglu, Ph.D. dissertation, Massachusetts Institute of Technology, 2007.
[2]A. A. Zbib, S. D. Mesarovic, E. T. Lilleodden, D. McClain, J. Jiao, and D. F. Bahr, Nanotechnology **19**, 175704 (2008).
[3]C. M. McCarter, R. F. Richards, S. D. Mesarovic, C. D. Richards, D. F. Bahr, D. McClain, and J. Jiao, J. Mater. Sci. **41**, 7872 (2006).
[4]M. Xu, D. N. Futaba, T. Yamada, M. Yumura, and K. Hata, Science **330**, 1364 (2010).
[5]S. Pathak, Z. G. Cambaz, S. R. Kalidindi, J. G. Swadener, and Y. Gogotsi, Carbon **47**, 1969 (2009).
[6]Y. Gogotsi, Science **330**, 1332 (2010).
[7]S. B. Hutchens, L. J. Hall, and J. R. Greer, Adv. Funct. Mater. **20**, 2338 (2010).
[8]A. Cao, P. L. Dickrell, W. G. Sawyer, M. N. Ghasemi-Nejhad, and P. M. Ajayan, Science **310**, 1307 (2005).
[9]M. R. Maschmann, Q. Zhang, R. Wheeler, F. Du, L. Dai, and J. Baur, ACS Appl. Mater. Interfaces **3**, 648 (2011).
[10]S. Mesarovic, C. Mccarter, D. F. Bahr, H. Radhakrishnan, R. Richards, C. Richards, D. Mcclain, and J. Jiao, Scr. Mater. **56**, 157 (2007).
[11]A. Qiu, D. F. Bahr, A. A. Zbib, A. Bellou, S. D. Mesarovic, D. McClain, W. Hudson, J. Jiao, D. Kiener, and M. J. Cordill, Carbon **49**, 1430 (2011).
[12]A. Misra, J. R. Raney, A. E. Craig, and C. Daraio, Nanotechnology **22**, 425705 (2011).
[13]Y. Won, Y. Gao, M. A. Panzer, S. Dogbe, L. Pan, T. W. Kenny, and K. E. Goodson, Carbon **50**, 347 (2012).
[14]X. Gui, A. Cao, J. Wei, H. Li, Y. Jia, Z. Li, L. Fan, K. Wang, H. Zhu, and D. Wu, ACS Nano **4**, 2320 (2010).
[15]J. R. Raney, F. Fraternali, A. Amendola, and C. Daraio, Compos. Struct. **93**, 3013 (2011).
[16]F. Fraternali, T. Blesgen, A. Amendola, and C. Daraio, J. Mech. Phys. Solids **59**, 89 (2011).
[17]S. B. Hutchens, A. Needleman, and J. R. Greer, J. Mech. Phys. Solids **59**, 2227 (2011).
[18]A. Carlson and T. Dumitrică, Nanotechnology **18**, 065706 (2007).
[19]A. I. Zhbanov, E. G. Pogorelov, and Y.-C. Chang, ACS Nano **4**, 5937 (2010).
[20]M. F. De Volder, D. O. Vidaud, E. R. Meshot, S. Tawfick, and A. J. Hart, Microelectron. Eng. **87**, 1233 (2010).
[21]L. J. Gibson and M. F. Ashby, *Cellular Solids: Structure and Properties*, 2nd ed. (Cambridge University Press, Cambridge, UK, 1999).
[22]J. D. van der Waals, Ph.D. dissertation, University of Leiden, 1873.